Chinese Chemical Letters 34 (2023) 107655

Contents lists available at ScienceDirect

Chinese Chemical Letters

journal homepage: www.elsevier.com/locate/cclet

In situ monitoring of Suzuki-Miyaura cross-coupling reaction by using surface-enhanced Raman spectroscopy on a bifunctional Au-Pd nanocoronal film

Cancan Zhang, Yonglong Li, Aonan Zhu, Ling Yang, Xiaomeng Du, Yanfang Hu, Xian Yang, Feng Zhang, Wei Xie*

Key Laboratory of Advanced Energy Materials Chemistry (Ministry of Education), Tianjin Key Lab of Molecular Recognition & Biosensing, Haihe Laboratory of Sustainable Chemical Transformations, Renewable Energy Conversion and Storage Center, College of Chemistry, Nankai University, Tianjin 300071, China

ARTICLE INFO

Article history:
Received 29 April 2022
Revised 17 May 2022
Accepted 30 June 2022
Available online 2 July 2022

Keywords:
Suzuki-Miyaura cross-coupling reaction
Au-Pd
SERS
In situ monitoring
Kinetics

ABSTRACT

Surface-enhanced Raman spectroscopy (SERS), a powerful surface vibrational spectroscopic technique, is ideally suited for *in situ* monitoring the chemical transformations occurred at surfaces and/or interfaces. For *in situ* SERS monitoring, a platform integrated both plasmonic and catalytic activity is a prerequisite. Here, we fabricate a bifunctional Au-Pd nanocoronal film for *in situ* SERS monitoring Suzuki-Miyaura cross-coupling reaction. This excellent bifunctional substrate leads to the coupling of high catalytic activity with a strong SERS effect at the center of two adjacent Au cores and shows fine reproducibility and stability of SERS signals. During investigating the Suzuki reaction with *in situ* SERS, we found two distinct catalytic kinetic processes resulted from two disparate catalytic sites on a Au-Pd nanocoronal. Comparing with conventional analytical techniques, this work provides a novel approach for studying Suzuki reactions at surfaces and/or interfaces with *in situ* SERS.

Surface-enhanced Raman spectroscopy (SERS), based on the localized surface plasmon resonance (LSPR) effect, can provide us significantly enhanced fingerprint vibrational information of molecules adsorbed on the surface [1–7]. In recent years, SERS has been a powerful pathway to *in situ* monitor interfacial reactions [8–14]. For instance, Kneipp *et al.* demonstrated that the kinetics of catalyzed reactions can be determined with *in situ* SERS by just mixing the catalysts in proximity to aminosilane-immobilized Au nanoparticles (NPs) [8]. Schlücker and other workers succeeded in the label-free *in situ* SERS monitoring of 4-nitrothiophenol (4-NTP) reduction catalyzed by small SERS-inactive Au NPs and circumventing the hot-electrons-induced side reactions with a single bifunctional 3D superstructure (Au@SiO_2@satelite-Au) [15]. Han *et al.* distinguished different catalytic sites for 4-NTP reduction on a complexed nanorod (Au nanorod@AuPd) with *in situ* SERS monitoring, which exemplifies exciting prospects for studying catalytic reaction processes on catalyst surfaces with high sensitivity [16]. Except for the reduction of 4-NTP, Weckhuysen *et al.* firstly extended the *in situ* SERS monitoring to the sequential hydrogenation of phenylacetylene on the surface of Au@SiO_2@satelite-Pt, in which they observed the sequential hydrogenation of phenylacetylene into styrene and ultimately ethylbenzene with hydrogen [16].

Generally, a requisite of *in situ* SERS monitoring catalytic reactions is the construction of an appropriate bifunctional platform possessing both plasmonic and catalytic activity [8,15,18-21]. To date, several kinds of bifunctional nanostructures have been developed, such as core@shell [22–27], shell-isolated nanoparticle (SHIN)@satelites [15,17,28-32], and other hierarchical structures [33–35]. In practical catalysis, hierarchical structures with exposure of two or more metals usually perform better activity. However, the current applications of these materials in SERS are few and still limited to the model reaction (hydrogenation reduction) [33]. Few SERS investigations on other organic reactions are reported. In 2019, our group first reported *in situ* SERS characterization of the Suzuki-Miyaura cross coupling reaction (Suzuki reaction for short) catalyzed by Pd [36]. This work not only extended the range of *in situ* SERS monitoring, but also provided solid evidence for the catalysis mechanism on Pd NPs. Subsequently, Ren group utilized *in situ* SERS to monitor the Suzuki reaction catalyzed by Au@Pd NPs and confirmed the hot electron transfer mechanism according to the linear relationship between the reaction rate and laser power [22]. Apart from the both, there is no investigation about the Suzuki reaction proceeding on hierarchical catalysts, which is of significance for practical catalysis applications.

* Corresponding author.
E-mail address: wei.xie@nankai.edu.cn (W. Xie).

https://doi.org/10.1016/j.cclet.2022.06.078
1001-8417/

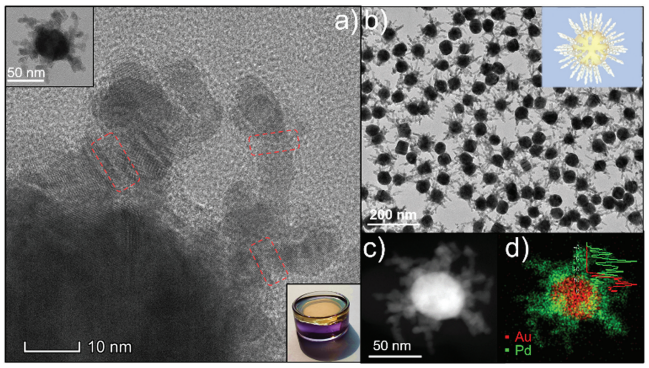

Fig. 1. (a) HRTEM of Au-Pd nanocoronals (the top left inset is the corresponding single Au-Pd nanocoronal; the red dashed circles exemplify the OA sites of Pd growth; the inset in the bottom right is the photo of Au-Pd nanocoronal film fabricated by slightly modified LB method). (b) The TEM images of Au-Pd nanocoronal monolayer film (the top right inset is the 3D model of single Au-Pd nanocoronal). (c) HADDF-STEM and (d) EDS mapping of Au-Pd nanocoronals.

Here, we fabricated a kind of peculiar Au-Pd hybrid NPs by using Au spheres (50.2 ± 5.0 nm) (Fig. S1 in Supporting information) as seeds and Na_2PdCl_4 as the precursor of Pd, which featured dozens newly grown Pd coronals with about 43.6 ± 6.3 nm length and 9.5 ± 1.7 nm width on Au NPs (Fig. 1). Therefore, it will be termed as Au-Pd nanocoronals in the following. The appearance of many defect sites indicated that the growth of Pd coronals followed the successive oriented attachment (OA) mechanism (dashed circles in Fig. 1a) [37,38], which will greatly improve the catalytic performance of Au-Pd nanocoronals. Because it has been proved that defect sites always are the active center of catalysis. To clarify the separate and exposed Au and Pd phases, we took HAADF-STEM as shown in the Fig. 1c, in which dozens separate Pd coronals can be easily distinguished from the Au cores in the center regions by the obvious different contrast of Au and Pd. The gaps between Pd coronals with darker contrast suggested that both independent Au and Pd phases are exposed. Combined EDS elemental analysis with HAADF-STEM (Figs. 1c and d), we can depict the three-dimensional nanostructure of Au-Pd nanocoronals as shown in the inset of Fig. 1b.

It has been reported that the agglomeration of particles can result in the improved SERS enhancement due to the considerably plasmonic coupling among particle junctions, known as "hot spots" [1,39,40]. In order to obtain fine and reproducible SERS signals, we assemble the Au-Pd nanocoronals into a film with the slight modified Langmuir-Blodgett (LB) method as the SERS monitoring platform. Briefly, owing to the tension in water-oil interface, Au-Pd nanocoronals simultaneously assemble into a monolayer film, which can be visualized by the glittering film at the interface shown in the bottom right inset of Fig. 1a. The TEM of the Au-Pd nanocoronal film indicates a monolayer film is formed (Fig. 1b).

Prior to *in situ* monitoring the Suzuki reaction with SERS, it is necessary to verify the bifunctionality of the prepared SERS substrate. At first, the SERS activity is confirmed by measuring the SERS spectra of 4-nitrothiophenol (4-NTP), known as a probe molecule of SERS measurement. The three characteristic peaks of 4-NTP can be easily distinguished on Au-Pd nanocoronals including 1079 cm^{-1}, 1330 cm^{-1} and 1576 cm^{-1}, respectively assigned to the C-S stretching, O-N-O stretching and the phenyl-ring mode [15,18,41-43]. Compared with the Raman spectra on Au NPs (black line in Fig. 2a), the noise ratio on Au-Pd nanocoronals is a little damped but still enough clear for the SERS detection. Furthermore, the distribution of enhanced localized electromagnetic fields is depicted by the three-dimensional finite difference-time domain (3D-

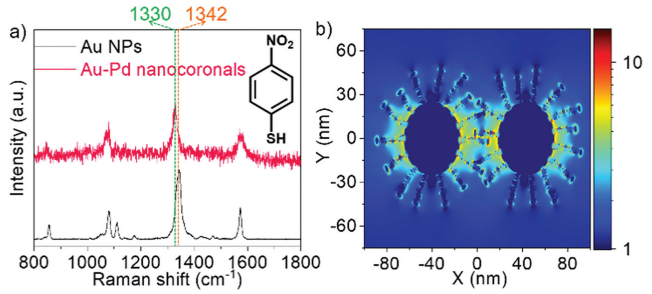

Fig. 2. (a) The SERS spectra of 4-NTP on Au NPs and Au-Pd nanocoronals with the same measure conditions. (b) The distribution of enhanced electromagnetic field simulated by FDTD.

FDTD) simulation. The simulation result in Fig. 2b shows that enhanced localized electromagnetic fields mainly distribute around the surrounding within 20 nm of Au-Pd nanocoronals and the closer to the surface of Au core, the brighter color indicating the stronger the enhancement effect. What is more, little enhanced field in the direction perpendicular to the incident light source is observed, which manifests the SERS activity of Au-Pd nanocoronals is mostly contributed by the LSPR effect. Consequently, we can achieve a SERS detection with Au-Pd nanocoronals by exciting the LSPR effect and plasmonic coupling between nanostructures to generate highly enhanced field around them.

Apart from the fine SERS activity, catalytic activity is the other requisite for a bifunctional SERS substrate. Given the reduction of 4-NTP is the most commonly used model reaction for *in situ* SERS monitoring, we also utilize it to validate the bifunctionality of the above SERS substrate. The reaction can be on-site completed within dozens of seconds upon the introduction of hydrogen and the whole reaction process can be clearly monitored (Fig. S2a in Supporting information). While the reaction can not occur on pure Au NPs concluded by no SERS signals belonging to products detected even when the reaction time is tripled (Fig. S3 in Supporting information). Thus, the above results evidence the excellent dual function of the Au-Pd nanocoronal films, SERS and catalytic activity.

For the exploration of reaction mechanisms by *in-situ* SERS monitoring, stability and reproducibility of signals collected on the substrate are of critical importance. In order to make an assessment for the as-prepared Au-Pd nanocoronal films, the characteristic peak at about 1330 cm^{-1} of 4-NTP is chosen to obtain the SERS mapping within a 20×20 μm^2 area. From the mapping result (Fig. 3), it is reasonable to conclude that SERS signals on the self-assembly Au-Pd nanocoronal film (Fig. 3b) are superiorly

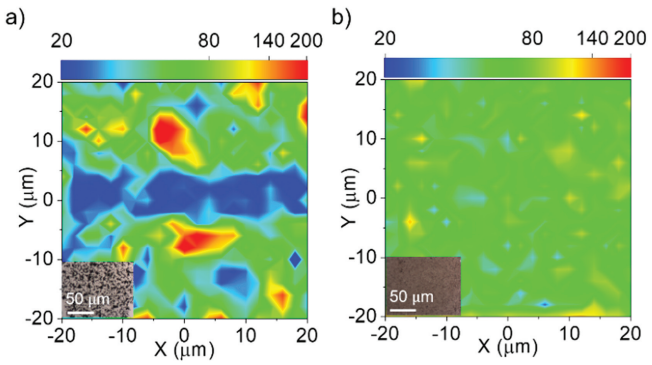

Fig. 3. SERS mapping of 4-NTP over a 20×20 μm^2 area on the Au-Pd nanocoronal films by dropping (a) and self-assembly (b) using the band at 1330 cm^{-1} (the inset photos are taken by LabRAM HR Evolution microscope (Horiba Jobin Yvon) equipped with a 50× objective).

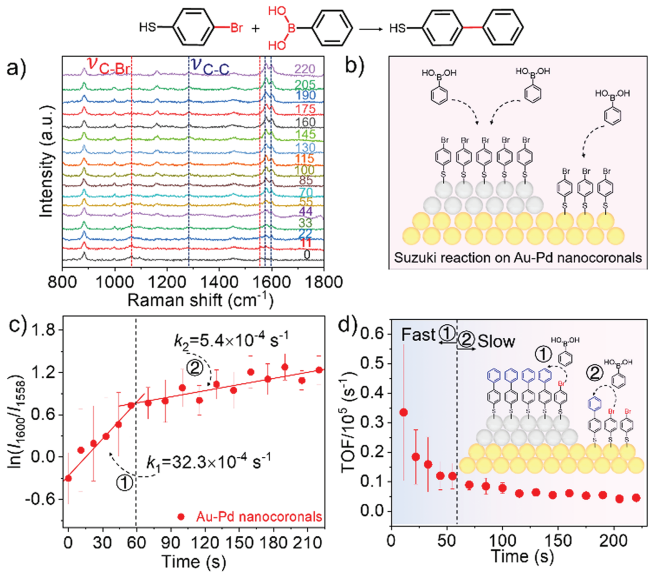

Fig. 4. (a) SERS spectra at different reaction time by *in situ* monitoring the Suzuki reaction on Au-Pd nanocoronals precoated with 4-BTP. (b) Sketch map for the reaction process. (c) A plot of the logarithm of the area ratio at 1600 and 1558 cm^{-1} *versus* reaction time ($\ln(I_{1600}/I_{1558}) \sim t$). (d) The time dependency plot of (TOF/10^5) for the Suzuki reaction of 4-BTP on Au-Pd nanocoronals.

stable and reproducible, especially, compared with the signals obtained on the dropped samples in Fig. 3a. In addition, the SERS signals on the former follow normal distribution with a standard deviation of 17.5% (Fig. S4 in Supporting information). Furthermore, the results of statistic method—*t* test validate the reproducibility of SERS signals collected on the Au-Pd nanocoronal films from different batches (details in Supporting information).

With the above fabricated bifunctional SERS substrate, the kinetics of Suzuki reaction was monitored by *in situ* SERS. The progress of the Suzuki reaction catalyzed by Au-Pd nanocoronals is traced by the time series of *in situ* SERS spectra of 4-bromothiolphenol (4-BTP) adsorbed on the Au-Pd nanocoronals immersed in the ethanol solution of $PhB(OH)_2$ (Fig. 4a). It should be noted that the remaining 4-BTP molecules have been removed by centrifuging and washing with ethanol and water prior to fabricating films, which ensures that all the SERS signals are from the molecules adsorbed on the surfaces of Au-Pd nanocoronals. From the dynamic SERS spectra in Fig. 4a, the characteristic peaks of 4-BTP can firstly be detected at 1065 cm^{-1} and 1560 cm^{-1}, which is attributed to a hybrid mode of phenyl ring and C-Br bond vibrations and the symmetric stretching mode of the phenyl ring, respectively [22,36]. Once initiating the SERS monitoring, the peaks associated with 4-BTP decreased and three new peaks at 1283, 1580 and 1600 cm^{-1} become appeared within 10 s, which are the characteristic peaks of 4-mercapto-biphenyl (4-MBP) and should be assigned to the stretching between two phenyl rings, the symmetric stretching modes of the two phenyl rings [22,36]. The whole conversion ultimately completes within 220 s, the transformation process of which can be captured thanks to the fast and sensitive characteristics of SERS. Additionally, no cross-coupling products is detected in the case without $PhB(OH)_2$ or Pd (pure Au NPs), results of which are shown in Figs. S5a and b (Supporting information). All these results demonstrate that it exactly is the Suzuki reaction that is catalyzed by palladium (Fig. 4b).

To decipher the reaction kinetics on Au-Pd nanocoronals, the integral area ratio of SERS peaks at 1600 and 1558 cm^{-1} (denoted as I_{1600} and I_{1558}) is tracked, which is proportional to the surface coverage percentage (θ) of the cross-coupling products (4-MBP) since a monomolecular layer of 4-BTP originally forms on the surface of Au-Pd nanocoronals through chemisorption [16,44,45]. Therefore, the surface coverage percentage θ of 4-MBP can be calculated by $\theta_{4\text{-MBP}}(t) = I_{t\text{-}1600}/I_{t\text{-}1558}$. Then, the equation of turnover frequency (TOF) normalized to the fraction of Pd active sites at the catalyst surface, derived from the atomic ratio of Pd and Au in XPS (Fig. S6 in Supporting information), can be expressed as the following (Eq. 1):

$$\mathrm{TOF}\ (\mathrm{s}^{-1}) = -\frac{\partial(1-\theta_{[4\text{-MBP}]}(t))}{\partial t} \times \frac{1}{\eta} = k \times [\mathrm{PhB(OH)_2}]^m \times \left[1 - \theta_{[4\text{-MBP}]}(t)\right]^n \quad (1)$$

where m and n are the reaction order of [$PhB(OH)_2$] and [4-BTP], respectively. η is the fraction of Pd. Given the much excessive concentration of [$PhB(OH)_2$], Eq. 1 can be simplified into Eq. 2:

$$\mathrm{TOF}\ (\mathrm{s}^{-1}) = -\frac{\partial(1-\theta_{[4\text{-MBP}]}(t))}{\partial t}\frac{1}{\eta} = k \times \left[1 - \theta_{[4\text{-MBP}]}(t)\right]^n \quad (2)$$

Therefore, the reaction order of [4-BTP], n, can be obtained by plotting $\ln(-\frac{\partial(1-I_{t-1600}/I_{t-1580})}{\partial t}\frac{1}{\eta})$ *versus* $\ln(1-\frac{I_{t-1600}}{I_{t-1580}})$ (Fig. S7 in Supporting information), namely, $n = 0.76 \pm 0.15$, indicating the Suzuki reaction approximately follows the first-order kinetics. Then, Eq. 3 can be obtained:

$$\ln\left(\frac{I_{t-1600}}{I_{t-1580}}\right) = k \times \eta \times t \quad (3)$$

According to Eq. 3 the reaction rate constant can be derived from the linearly fitted slope of the $\ln(\frac{I_{t-1600}}{I_{t-1580}}) \sim t$ plot (Fig. 4c). Surprisingly, there is an inflection point in the time dependency plot of $\ln(I_{1600}/I_{1558})$ obtained on the Au-Pd nanocoronals (Fig. 4c). The obvious different kinetic processes indicate the coexistence of two kinds of catalytic sites with different activities on Au-Pd nanocoronals [16]. The both kinetic constants ($k_1 = 32.3 \times 10^{-4}$ s^{-1}, $k_2 = 5.4 \times 10^{-4}$ s^{-1}) numerically show that the second process is much slower than the first one. Combined with the nanostructure of Au-Pd nanocoronals, the two different kinetic processes are supposed to result from the reactions of 4-BTP on Pd and Au surfaces, respectively.

Taking the advantage of SERS as a powerful surface and interface molecular characterization technology, we further make a calculation according to the spatial distribution of molecular adsorption on Au-Pd nanocoronal surfaces. For the convenience of calculation, the coronal Pd and the core Au are respectively simplified as a cylinder (height: $h = 43.6$ nm, bottom diameter: $r = 9.5$ nm) and a sphere (diameter: $d = 50.2$ nm). According to the area formula and the numbers of coronal Pd, we can derive the numbers of 4-BTP adsorbed on Pd (N_{Pd}) and Au (N_{Au}) with the area occupied by a 4-BTP molecule ($S = 0.2$ nm^2). Therefore, TOF at each monitoring time can be calculated from the Eq. 4:

$$\mathrm{TOF}\ (\mathrm{s}^{-1}) = \frac{I_{1600}}{I_{1558}} \times (N_{Pd} + N_{Au}) \times \frac{1}{t} \quad (4)$$

Two different sections also can be distinguished in the Fig. 4d, the coincidence of which with the aforementioned discussion demonstrates the validity of our explanation. Moreover, it should be noted that the steric effect of the product 4-MBP also can be distinguished from the gradual decrease of TOF particularly on Pd.

It is reasonable that the faster process is assigned to the 4-BTP adsorbed on the Pd surface known as highly efficient catalyst for the Suzuki reaction. However, people may wonder how the 4-BTP adsorbed on inert Au surfaces is catalyzed into 4-MBP. According to reported works, palladium could leach in the means of atoms from the NPs or metal complexes through the oxidative addition of palladium and aryl halides [46–48]. The leached palladium species can reversibly form Pd NPs, the activity of which is reported to be

greatly decreased [49,50]. Besides that, it involves diffusion process, which further drags the reaction progress. Therefore, it is deduced that the second process could be the slower conversion of 4-BTP on Au surfaces catalyzed by the reformed Pd NPs with deteriorated activity, which becomes visible when the faster process on Pd is completed (as shown in the inset of Fig. 4d).

In summary, the bifunctional Au-Pd nanocoronals provide us an excellent platform for the *in situ* monitoring catalytic reactions with SERS. With the self-assembly Au-Pd nanocoronal films, we not only achieve fine SERS signals with good reproducibility, but also ascertain the kinetics of the Suzuki-Miyaura cross-coupling reaction catalyzed by Au-Pd nanocoronals. Two distinct kinetics processes rooted in the different catalytic activity of Au and Pd, are reflected by *in situ* SERS monitoring, which corroborates the ultrasensitivity of SERS for *in situ* monitoring reactions on the surface of nanocatalysts. This work provides a paradigm for the exciting prospect of SERS in exploring more practical catalytic reactions with superior sensitivity, which will be highly useful for deeply understanding catalytic mechanisms and reasonably optimizing catalysts.

Declaration of competing interest

The authors declare that they have no known competing financial interests or personal relationships that could have appeared to influence the work reported in this paper.

Acknowledgments

The authors acknowledge the financial support from the National Natural Science Foundation of China (No. 22022406), the Natural Science Foundation of Tianjin (Nos. 20JCJQJC00110 and 20JCYBJC00590), the 111 project (No. B12015), the Haihe Laboratory of Sustainable Chemical Transformations.

Supplementary materials

Supplementary material associated with this article can be found, in the online version, at doi:10.1016/j.cclet.2022.06.078.

References

[1] H.K. Lee, Y.H. Lee, C.S.L. Koh, et al., Chem. Soc. Rev. 48 (2019) 731–756.
[2] A.I. Pérez-Jiménez, D. Lyu, Z. Lu, G. Liu, B. Ren, Chem. Sci. 11 (2020) 4563–4577.
[3] Y.H. Wang, S. Zheng, W.M. Yang, et al., Nature 600 (2021) 81–85.
[4] C.L. Warkentin, Z.W. Yu, A. Sarkar, R.R. Frontiera, Acc. Chem. Res. 54 (2021) 2457–2466.
[5] S. Schlücker, Angew. Chem. Int. Ed. 53 (2014) 4756–4795.
[6] C.C. Zhang, Y.Y. Zhang, W. Xie, J. Energy Chem. 63 (2021) 40–53.
[7] Y.J. Zhang, Y.Z. Zhu, J.F. Li, Acta Phys. Chim. Sin. 37 (2021) 2004052.
[8] V. Joseph, C. Engelbrekt, J. Zhang, et al., Angew. Chem. Int. Ed. 51 (2012) 7592–7596.
[9] D. Glass, R. Quesada-Cabrera, S. Bardey, et al., ACS Energy Lett. 6 (2021) 4273–4281.
[10] P. Miao, Y. Ma, M.T. Sun, J. Li, P. Xu, Faraday Discuss. 214 (2019) 297–307.
[11] W.K.H. Ho, Z.Y. Bao, X. Gan, et al., J. Phys. Chem. Lett. 10 (2019) 4692–4698.
[12] D. Wang, F.X. Shi, J. Jose, et al., J. Am. Chem. Soc. 144 (2022) 5003–5009.
[13] R. Li, C.C. Zhang, D. Wang, et al., Chin. Chem. Lett. 32 (2021) 2846–2850.
[14] Y. Liu, J.Y. Cai, J.B. Zhou, et al., eScience 2 (2022) 389–398.
[15] W. Xie, B. Walkenfort, S. Schlücker, J. Am. Chem. Soc. 135 (2013) 1657–1660.
[16] J.H. Huang, Y.H. Zhu, M. Lin, et al., J. Am. Chem. Soc. 135 (2013) 8552–8561.
[17] C.S. Wondergem, T. Hartman, B.M. Weckhuysen, ACS Catal. 9 (2019) 10794–10802.
[18] W. Xie, C. Herrmann, K. Kompe, M. Haase, S. Schlücker, J. Am. Chem. Soc. 133 (2011) 19302–19305.
[19] H.S. Su, H.S. Feng, X. Wu, J.J. Sun, B. Ren, Nanoscale 13 (2021) 13962–13975.
[20] W. Xie, S. Schlücker, Rep. Prog. Phys. 77 (2014) 116502.
[21] S.Y. Ding, J. Yi, J.F. Li, et al., Nat. Rev. Mater. 1 (2016) 16021.
[22] H.S. Feng, F. Dong, H.S. Su, M.M. Sartin, B. Ren, J. Appl. Phys. 128 (2020) 173105.
[23] H. Zhang, J. Wei, X.G. Zhang, et al., Chem 6 (2020) 689–702.
[24] Y.J. Zhang, P.M. Radjenovic, X.S. Zhou, et al., Adv. Mater. 33 (50) (2022) e2005900.
[25] Y.H. Wang, X.T. Wang, H. Ze, et al., Angew. Chem. Int. Ed. 60 (2021) 5708–5711.
[26] H. Zhang, S. Duan, P.M. Radjenovic, Z.Q. Tian, J.F. Li, Acc. Chem. Res. 53 (2020) 729–739.
[27] Q.L. Cui, G.Z. Shen, X.H. Yan, et al., ACS Appl. Mater. Interfaces 6 (2014) 17075–17081.
[28] K.F. Zhang, L. Yang, Y.F. Hu, et al., Angew. Chem. Int. Ed. 59 (2020) 18003–18009.
[29] D.Y. Wei, M.F. Yue, S.N. Qin, et al., J. Am. Chem. Soc. 143 (2021) 15635–15643.
[30] J. Wei, S.N. Qin, J. Yang, et al., Angew. Chem. Int. Ed. 60 (2021) 9306–9310.
[31] C.S. Wondergem, J.J.G. Kromwijk, M. Slagter, et al., ChemPhysChem 21 (2020) 625–632.
[32] H. Zhang, C. Wang, H.L. Sun, et al., Nat. Commun. 8 (2017) 15447.
[33] J.M. Li, J.Y. Liu, Y. Yang, D. Qin, J. Am. Chem. Soc. 137 (2015) 7039–7042.
[34] X.H. Zhao, M. Deng, G.F. Rao, et al., Small 14 (2018) e1802477.
[35] Y. Yang, Q. Zhang, Z.W. Fu, D. Qin, ACS Appl. Mater. Interfaces 6 (2014) 3750–3757.
[36] Y.R. Zhao, L.L. Du, H.X. Li, W. Xie, J. Chen, J. Phys. Chem. Lett. 10 (2019) 1286–1291.
[37] R.H. Chen, Q.N. Nguyen, Y.N. Xia, ChemNanoMat 8 (2022) e202100474.
[38] A.G.M. Da Silva, R.H. Chen, Q.N. Nguyen, et al., Chem. Mater. 33 (2021) 8430–8439.
[39] J. Gargiulo, R. Berté, Y. Li, S.A. Maier, E. Cortés, Acc. Chem. Res. 52 (2019) 2525–2535.
[40] Y. Zhang, B. Walkenfort, J.H. Yoon, S. Schlücker, W. Xie, Phys. Chem. Chem. Phys. 17 (2015) 21120–21126.
[41] Y.Y. Dong, P. Jiang, W. Xie, Appl. Mater. Today 14 (2019) 201–206.
[42] Y.R. Zhao, R. Li, P. Jiang, et al., J. Phys. Chem. C 123 (2019) 15582–15588.
[43] W. Xie, S. Schlücker, Nat. Commun. 6 (2015) 7570.
[44] B.I. Rosario-Castro, E.R. Fachini, J. Hernández, M.E. Pérez-Davis, C.R. Cabrera, Langmuir 22 (2006) 6102–6108.
[45] C. Silien, L. Dreesen, F. Cecchet, P.A. Thiry, A. Peremans, J. Phys. Chem. C 111 (2007) 6357–6364.
[46] A. Balanta, C. Godard, C. Claver, Chem. Soc. Rev. 40 (2011) 4973–4985.
[47] Q. Gu, Q.H. Jia, J.J. Long, Z.W. Gao, ChemCatChem 11 (2019) 669–683.
[48] D.B. Pacardo, J.M. Slocik, K.C. Kirk, R.R. Naik, M.R. Knecht, Nanoscale 3 (2011) 2194–2201.
[49] M. Kolter, K. Koszinowski, Chem. Eur. J. 25 (2019) 13376–13384.
[50] D. Astruc, Inorg. Chem. 46 (2007) 1884–1894.